Presentation of Digital Radiographic Systems and the Quality Control Procedures that Currently Followed by Various Organizations Worldwide

Maria E. Lyra*, Sofia D. Kordolaimi and Aikaterini-Lampro N. Salvara

Department of Radiology, University of Athens, Athens, Greece

Abstract: In the last decades, computed radiography (CR) and direct digital radiography (DDR) are becoming more popular in relation to traditional film screen radiography. This derives mostly from the fact that digital image is prone to post- processing analysis and it can also be stored for future use. Various organizations have published protocols in which guidelines concerning quality assurance and acceptance tests for digital systems are referred. In this paper, diverse methods for quality assurance of digital radiographic systems are presented based on current published protocols, as the protocols of King's Centre for the Assessment of Radiological Equipment in the United Kingdom (KCARE), America's Association of Physicists in Medicine (AAPM) and Australian College of Physical Engineers in Medicine (ACPSEM). This review is also referred to other studies conducted from individual teams which either count on the mentioned protocols or they have chosen to follow an alternative method. Firstly, a brief description of CR and DDR systems based on the patents US 20050029475 (2005) and US 6944265 (2005) is presented. Subsequent to this, the control method of image presentation on monitors and printers is discussed by utilizing test patterns. Detector's dose efficiency is also depicted by using the detective quantum efficiency curve (DQE). Moreover, the entrance surface dose (ESD) and radiation output rate dose are presented using an equivalent of soft tissue phantom. The quality control procedures of the parameters that affect the final image, as kVp performance, accuracy, repeatability, dose detector index (DDI), uniformity, linearity, threshold contrast detail detectability (TCDD), image noise, limiting spatial resolution, resolution uniformity, spatial accuracy, spatial linearity, laser beam function, erasure thoroughness, signal to noise ratio (SNR) and contrast to noise ratio (CNR), are introduced, as well. Moreover, the phantoms used in clinical practice for the quality control of the digital systems are briefly presented. Lastly, the proper operation of the automatic exposure control (AEC) conditions is also discussed.

Keywords: Direct digital radiography (DDR), computed radiography (CR), quality control, signal to noise ratio (SNR), contrast to noise ratio (CNR), image noise, ghosting erase, test patents, CR reader, photostimulated storage phosphor (PSP), detective quantum efficiency (DQE) curve, automatic exposure control (AEC).

1. INTRODUCTION

During the last decade, the classical film-screen radiology is being replaced by the Digital Radiology (DR) because of its enormous benefits. In this technique the images can be taken and displayed immediately (a few minutes after the examination), and can be deleted (if the quality is not the desirable) or corrected (if any improvement in the image quality is needed) and subsequently sent to a network of computers (PACS) through which they can be used in any department, any time. The use of this modality prevents the large size of storage films in the hospital; and it is more convenient for the patient to carry only a small sized compact disk that will contain all of his examinations. By these systems, dark room or chemical products are not required any more, the images are printed by printers similar to those of a usual PC and this is a time and environmental gain.

The advent of cutting- edge technology, because of its complexity and its sensitivity to failure due to electronic components drifts, brings with it new challenges in terms of its control and quality assurance (QA). Quality Control (QC) is an important part of a quality assurance (QA) program, in order to avoid unnecessary high doses and help to achieve better image quality. A sufficient number of national and international recommendations and protocols (KCARE, AAPM, ACPSEM, IAEA) that get involved with the QC of digital and computed radiography have been published. These protocols set tolerance levels for the various tests that are made for the X-ray tube and generator, X-ray tube control system, display station, image quality and patient dose.

This review starts with a brief reference to both digital and computed radiology and makes a comparison between them; then it focuses on the quality control (QC) of the computed radiology. It is necessary to become clear that the term 'digital radiography' encompasses the term 'computed radiography' but is also encompasses the 'direct digital radiography' (DDR) which is another digitalized technique referred in this review. Based on national and international protocols, the steps for an effective QC, the equipment that is used for the measurements and the tolerance levels are mentioned. It must be noticed that there is no reference to the quality control of the printed images (hard copy) as the image display on monitors is of greater importance, in digital

*Address correspondence to this author at the Department of Radiology, University of Athens, Athens, Greece; Tel: 0030- 210- 7286243; Fax: 0030-210-9827768; E-mail: mlyra@medimaging.gr

1877-6132/10

radiography. At the end of this review, a list of all the abbriviations mentioned in the text is displayed in the appendix.

2. COMPUTED RADIOGRAPHY AND DIRECT DIGITAL RADIOGRAPHY SYSTEMS

2.1. Computed Radiography (CR) systems

Computed Radiography (CR) is a process for capturing digital radiographic images. CR technology has been around since the early 1980s and has been widely accepted as a digital image acquisition process that produces images equivalent to conventional x-ray film-screen systems. For exposure, a storage phosphor plate (a photo-stimulable plate, or PSP) is placed in an x-ray cassette, instead of an X-ray film sheet. The storage phosphor plate fits inside a standard film cassette and is exposed to x-rays exactly like film. The image formation in CR systems is shown in Fig. (**1**).

Storage phosphor plate looks like the intensifying screen found in conventional film-screen cassettes. However, instead of emitting light immediately when exposed to x-rays, they have the special property of storing the x-ray energy in a latent image. This latent image is "developed" in a CR reader, when the phosphor plate is scanned by a light beam, such as a laser beam (Fig. **2**). The laser beam causes the storage phosphors to release UV light energy they have captured, in a photo-stimulable process. The CR reader extracts the information stored in the plate and this energy is converted into a digital image [1].

CR is preferable than the conventional x-ray film-screen systems as it eliminates the need for re-takes, eliminates lost images, simplifies the filing of images, and increases the capability for consultation made possible by electronic transmission of digital images. Storage phosphors are also unique because they respond to a very wide dynamic range of x-ray exposures. This latitude gives flexibility in selecting the appropriate x-ray technique without worrying about under- or over- exposure. Regardless of the exposure, the image can be displayed in an optimal mode. As a consequence, retakes due to inappropriate exposures are drastically reduced.

After exposure and scanning, the phosphor plate is "erased" by exposing it to bright light. The residue of the previous latent image in the phosphors is removed, and the plate is ready to be exposed again. The life of a phosphor plate depends on how carefully it is handled. Physical damage to the plate will limit its useful life. There is nothing about the chemistry of the phosphors that degrades after repeated exposures. If properly cared for, a plate will produce thousands of images. In factory tests, a single plate

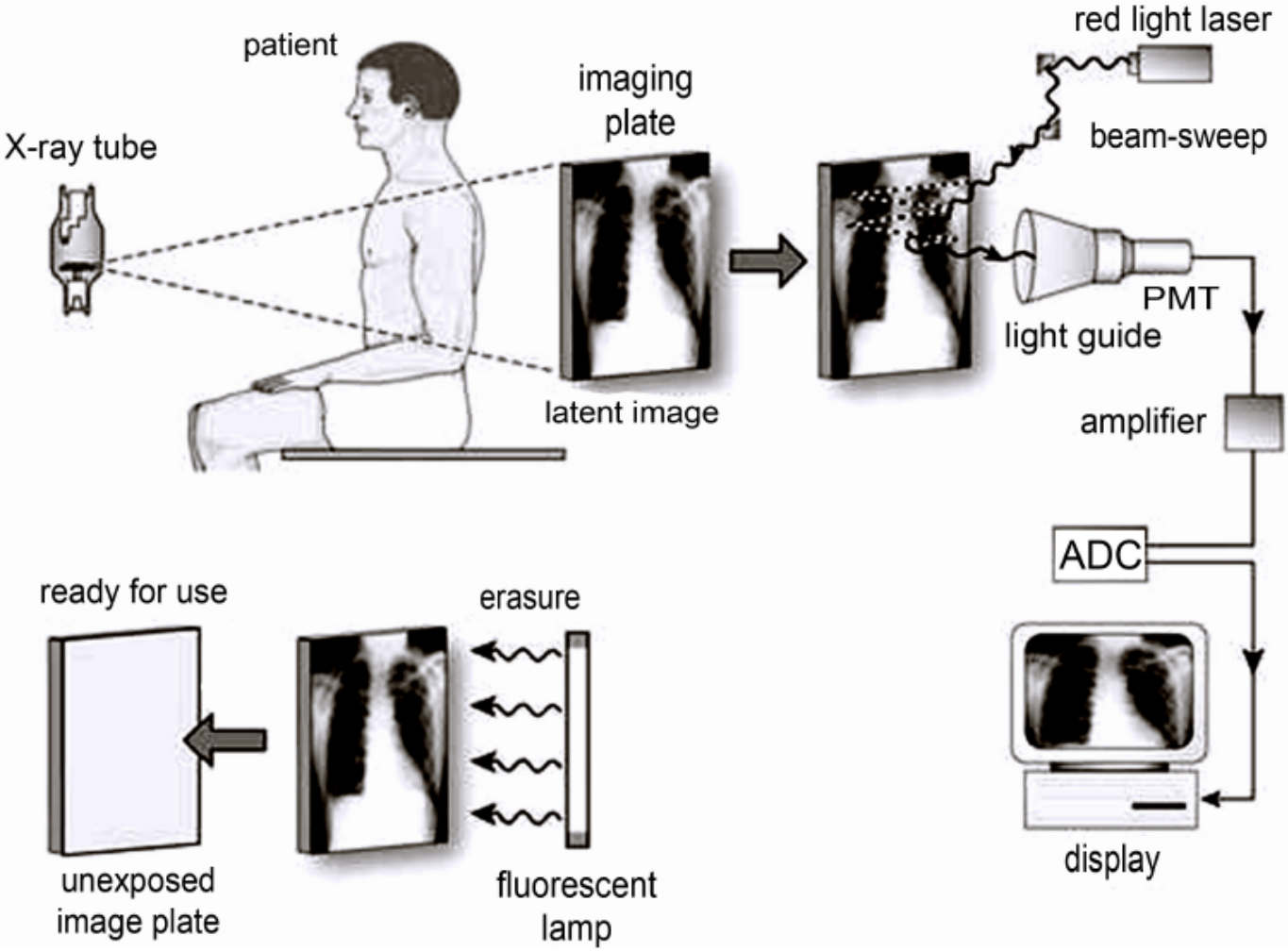

Fig. (1). Image formation in CR [1].

is scanned more than 10,000 times and is still in excellent condition. However, in conventional CR readers, the PSP is removed from the cassette before being inserted into the reader. In readers with rollers, the roller grabs the plate and can bend or rub the material, leading to reduced lifetime and image quality. Accordingly, two types of plates are currently in use- a substantially stiff plate which is difficult to bend, and a flexible plate which can be bent onto a cylinder for reading [2].

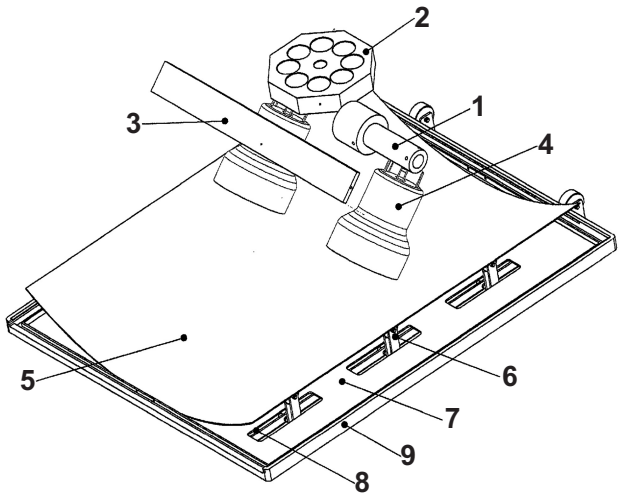

The CR reader consists of a stimulating beam source (**1**), mirrors (**2**, **3**), a photomultiplier (**4**), a stimulable phosphor sheet (**5**), a cassette (**7**), a base (**9**) which cooperates PSP with a lifting mechanism (**6**) and slots (**8**) [2].

Fig. (2). A schematic perspective view of a CR reader.

2.2. Direct Digital Radiography (DDR) Systems

The DDR system includes an x-ray source and an x-ray detector capable of automatic digital imaging without the use of an image intensifier. The detector detects the x-rays transmitted from the x-ray source through a subject of interest. Due to the limited dimensions of the detector's window, the position of the detector should change in order to receive a number of observable areas, known as fields of view (FOVs). The creation of a composite image is usually accomplished by having a system for acquiring images with a total FOV larger than the detector's. As illustrated in Fig. (**3**), the x-ray beam passes through an object of interest positioned on the radiographic table and impinges upon the detector, which converts the radiation into electric signal. This signal is then sent to the image storage enabling unit (computer workstation), which enables pre-processing operations and, subsequently, the storage of the image. At that point the image is elaborated and then sent to the image storage enabling unit to be printed on a film or saved in a compact disk.

Analytically, the function of the system is shown in the blog diagram in Fig. (**4**).

There are two types of digital image capture devices that are used, nowadays, in DDR. These devices include Flat Panel Detectors (FPDs), and High Density Line Scan Solid State detectors.

2.2.1. Flat Panel Detectors (FPDs)

FPDs [3] are classified in two main categories: Amorphous Silicon (a-Si), which is the most commonly used or amorphous Selenium (a-Se). The FPD in Fig. (**5**) includes an Amorphous Silicon Array (1) which is made of

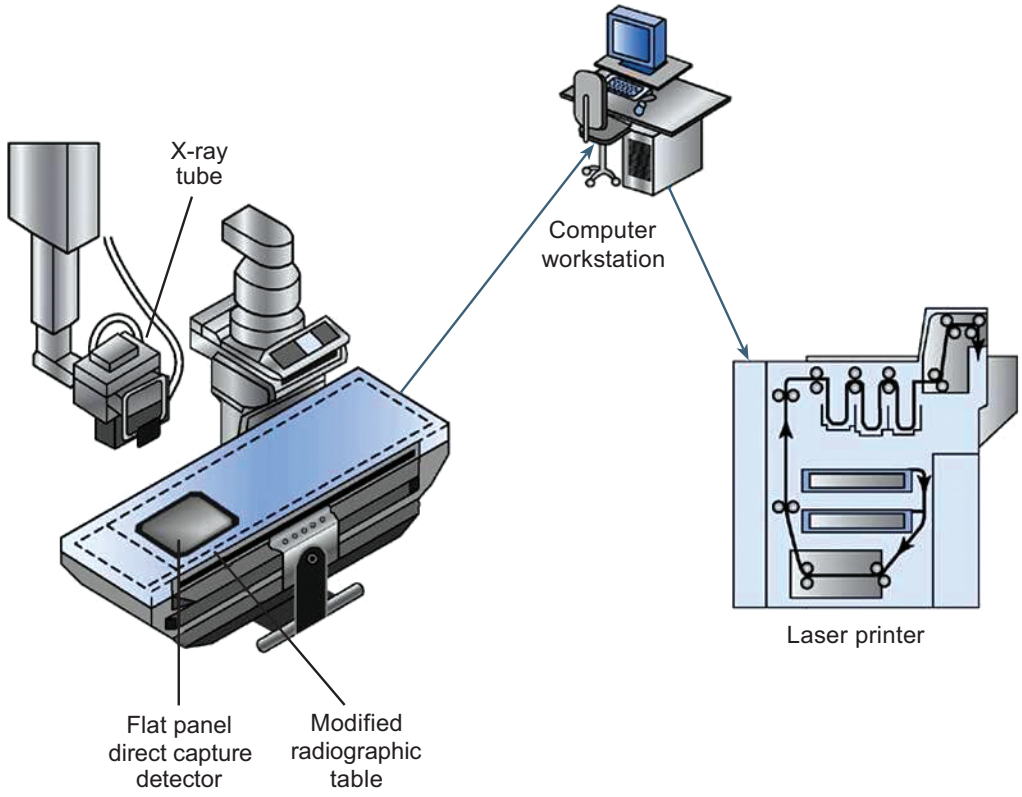

Fig. (3). Direct digital radiography.

amorphous silicon diodes and thin-film transistors (TFTs). Utilizing thin film, layers of amorphous silicon and various metals and insulators are deposited on a glass substrate (2) to form an Amorphous Silicon Array of photodiodes and a TFTs matrix, as well as the interconnections (3), and the contacts (4) on the edges of the panel. The scintillator (5), which converts x-ray photons into visible light photons, is made of Cesium Iodide and is deposited directly on top of the Amorphous Silicon Array. Schematically, the operation of the flat- panel detector is shown in Fig. (**6**).

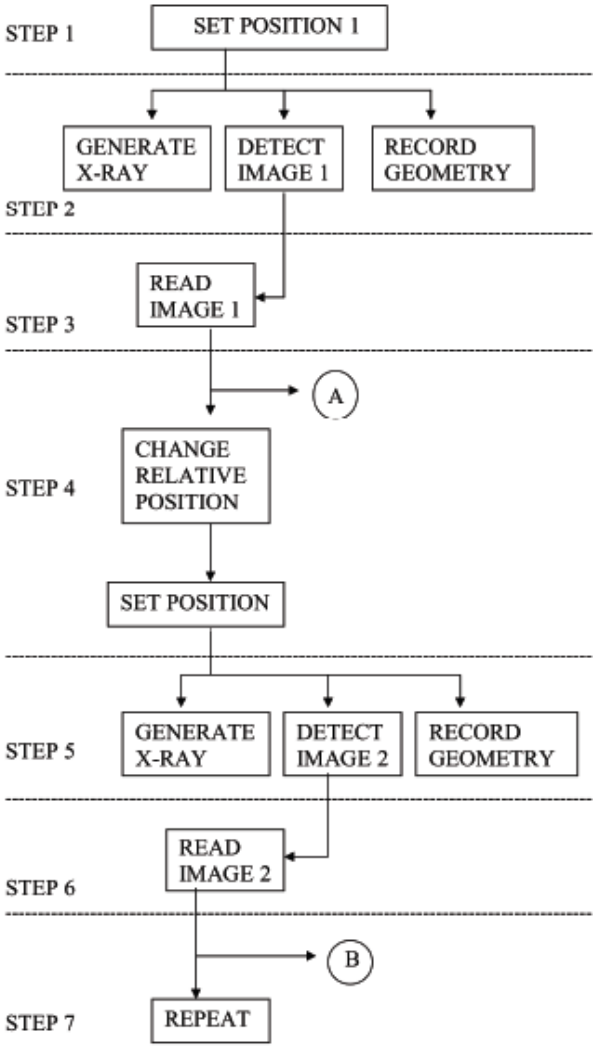

An initial position is set, the geometry is recorded by the positioner and the inclinometer, and then an x-ray is generated. When passing through the object the image is detected by an x-ray detector and is read by its electronics. Once the image is read it is sent to the processor. After the initial image is recorded, the position change mechanism modifies the relative position between the x-ray detector and the subject of interest and the subsequent position is then set. The x-ray source generates an x-ray and the detector detects a new image. The geometry of the second position is also recorded by the positioner and inclinometer. The image is then read by the x-ray detector electronics and the image is sent to the processor. If more than two images are desired, the process can be repeated to gather more images.

Fig. (4). A block diagram of the system function shows the various procedure steps.

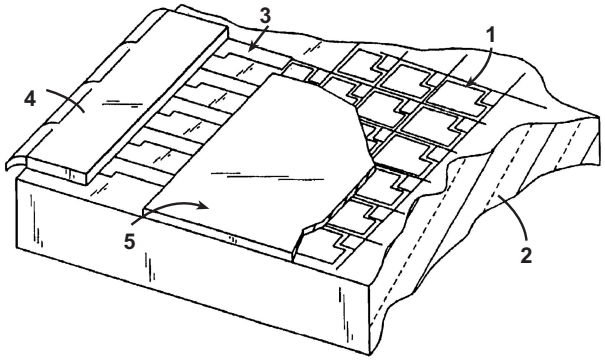

The detector consists of an Amorphous Silicon Array (**1**), a glass substrate (**2**) to form an Amorphous Silicon Array of photodiodes and a TFTs matrix, the interconnections (**3**), the contacts (**4**) on the edges of the panel and the scintillator (**5**) made of Cesium Iodide, which converts x-ray photons into visible light photons [3].

Fig. (5). The structure of a possible flat-panel x-ray detector.

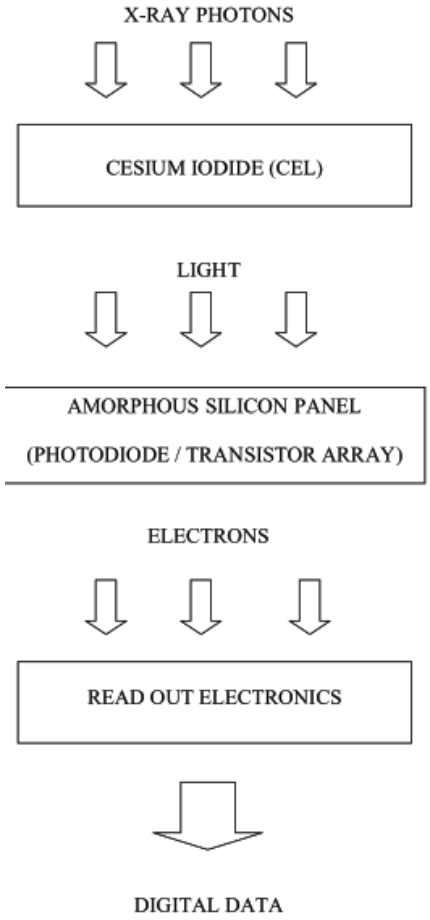

The system converts the X-ray energy to light when falling into the Cesium Iodide scintillator. The light is then channeled through the Amorphous Silicon photodiode array where it causes the charge of each photodiode to be depleted in proportion to the light it receives and is converted to a digital output signal, which is then read out by Thin Film Transistors (TFT's) or by fiber coupled Charged Couple Devices (CCD's). The image data file is sent to a computer for display and elaboration.

Fig. (6). A block diagram of the operation of the flat- panel detector [3].

The other type of FPD is a direct conversion type that uses a Selenium Array (instead of the Silicon Array) and is made of selenium diodes and thin-film transistors. The use of selenium obviates the need for a scintillator because the selenium converts directly the x-ray radiation into electonic signal. As a result the light scatter problem is tottaly avoided and it permits real-time readout. In comparison to other types of FPD, the Selenium Array gives very high modulation transfer function (MTF) and spatial resolution. However its application is limited to x-ray energy less than 150 keV and is mainly used in medical applications [4].

2.2.2. High Density Line Scan Solid State detectors

This type of detector is composed of Cesium Bromide (CsBr) phosphor. The phosphor detector records the X-ray energy during exposure and is scanned by a linear laser diode to excite the stored energy which is released and read out by a digital image capture array of Charge Coupled Devices (CCD's). The image data file is transmitted to a computer for further interpretation.

2.3. Comparison Between CR and DDR

Comparing CR and DDR systems it is clear that both have their advantages and disadvantages. DDR systems transfer the X-ray directly to a digital signal while CR systems get the X-ray image transferred to the plate, and from the plate, to the reader. There are clear-cut advantages to DDR from the standpoint of work flow as the reading procedure is omitted. Manual handling of the cassette housing the IP, in a CR system, is considered a disadvantage versus DDR but, on the other hand, this offers more flexibility in patient positioning. Another beneficial point for CR is that upgrading the existing equipment to CR is much more economical than the entire replacement of the whole X-ray imaging system with a DDR system. DDR algorithms also are not as sophisticated and fully worked out as CR. The reason for this may be the increased demand of CR systems upon DDR systems.

3. IMAGE PRESENTATION ON MONITORS AND PRINTERS

A very useful and necessary control of a DR system (CR or DDR) is to test the quality of the image presentation on monitors and printers. Quick tests of monitors and printers on a regular basis are required to detect electronic instabilities, film artefacts and printer artefacts. These tests are made by using test patterns, such as SMPTE or the TG18 (as shown in Fig. **7**), on each of the monitors used for reporting clinical images.

The system must be able to differentiate all the lines, from thick to narrow and both horizontally and vertically.

The test patterns are exposed on each monitor to ensure that [5-7]:

- All borders are visible and the resolution at all corners and in the middle is uniform
- The lines are straight and the squares appear as squares
- The ramp bars appear continuous without any contour lines or smearing and bleeding at black-white transitions
- The resolution bars everywhere on the pattern must not differ more than 20%
- All corner patches are visible and the squares of different shades from black to white are distinct,

(**a**) SMPTE test pattern

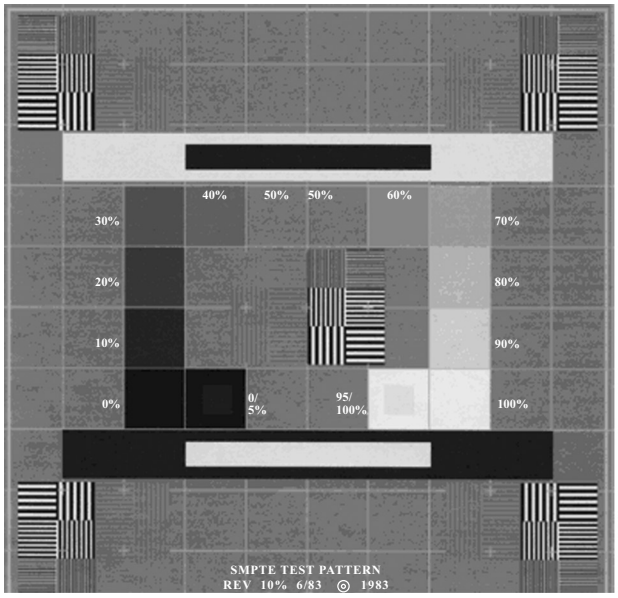

(**b**) TG18 test pattern

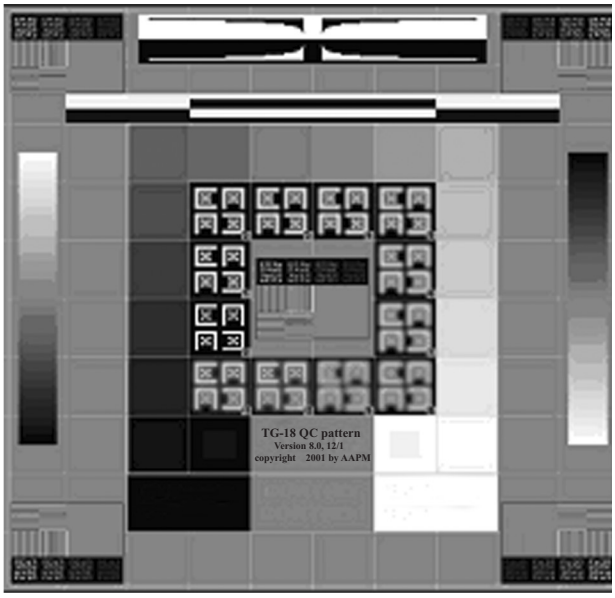

The test patterns are consisted by small squared areas (patches) that have a different range of grey colour. Each one of the 0% and 100% squares contain smaller squares that represent signal level steps of 5% and 95%, respectively. In the centre and at the edges of the patterns there are high contrast bar patterns of black and white pairs. These high contrast bar patterns are 6 squares filled with varying widths of alternating black/white horizontal and vertical lines.

Fig. (7). Two different types of test patterns that are being used to check the image presentation on monitors and printers.

- The 5% and 95% pixel value squares are clearly visible and differentiated from the larger squares 0% and 100% that contains them
- The pattern is centred in the active area
- No disturbing artefacts are visible
- Contrast response should not deviate from the DICOM Grayscale Standard Display Function (GSDF) contrast values by more than 10%.

The results of the measurements and the visibility are expected to be better if the ambient light is reduced. Ambient lights should not be turned off completely nor turned up completely. About 25 to 40 lux is generally sufficient to avoid most reflections and still provide sufficient light for the visual system to adapt to the surrounding environment and the displays [8].

Regarding the luminance of the monitors, the maximum luminance used for viewing digital conventional radiographs should be at least 200 cd/ m^2. Smaller ranges could lead to inadequate levels of contrast in displayed images, while larger values could lead to poor visualization of details, because of the limited range of the contrast sensitivity of the human eye. According to AAPM Task Group 18 recommendations, a high display contrast ratio with a low minimum luminance level (0.5 cd/ m^2) is most desirable [8, 9].

According to the European Reference Organization for Quality Assured Breast Screening and Diagnostic Services (EUREF) [10] and the Australian College of Physical Engineers in Medicine (ACPSEM) [5], this type of measurements is recommended to be made each week, while additional test patterns should be viewed on a monthly basis as proscribed by the monitor manufacturer's QC program or by the AAPM.

In order to check the optimal function of the printers and the quality of the image presentation on them, test patterns are used to test geometrical distortion, contrast visibility, printer artefacts, density response and uniformity. The test patterns are print-out and the medical physicists, in association with the relevant supplier engineer, are monitoring for changes in geometric distortion, contrast visibility, resolution, optical density range and artefacts. The parameters that are checked are the same as the ones for the monitors' displays. According to the ACPSEM, conformance with the Gray Scale Display Function (GSDF) can be determined by printing the TG18-PQC test pattern and measuring the optical densities (OD) of the marked regions. In addition, measurements are made, with the use of a densitometer, in order to calculate the mid density (MD) and the density difference (DD) and to ensure that they are within ± 0.15 OD of their baseline values. It is also needed that the sum of Base + Fog (B+F) should be within ± 0.03 OD and the maximum density (D_{max}) within ±0.10 OD, of their respective baseline values [5]. The 100% patch is the sum of the base, plus and fog, while the 40% patch is the index of the printer's speed. The contrast index of the printer is given by the subtraction of the OD of 10% and 70% patches [11].

In case of a softcopy image, it is necessary to measure and record the average pixel value by using the region of interest analysis (ROI). On the other hand, in case of a hardcopy (film) image the sensitometry strip must be printed and the summation of the base and the fog OD must be measured; the average OD ought to be measured as well.

4. DOSE EFFICIENCY

Dose efficiency is the parameter that relates to how effectively the detector uses the radiation that impinges upon it. In order to estimate the value of the dose efficiency it is necessary to measure the dose, the image resolution and noise under the same circumstances of section thickness, scan field and scan diameter. The dose efficiency of a detector can be characterized using the Detective Quantum Efficiency curve (DQE), which is a parameter that can be determined experimentally (though it is quite difficult to make experimental measurements), provides information about the additional noise added to the signal at all stages of its processing. It includes the contributions of all stages of the signal conversion, making it possible to compare on a quantitative basis different systems for X-ray imaging [12]. The DQE for the spatial frequency (u) along the horizontal or vertical direction (along the lines or rows of the pixel matrix of the detector) is determined using the following defining equation:

$$DQE(u) = MTF^2(u) \cdot \frac{W_{in}(u)}{W_{out}(u)}$$

where,

DQE(u): is reported at frequency multiples of 0.5 mm^{-1} up to the Nyquist frequency.

MTF(u): the modulation transfer function of the detector,

Win (u): the noise power spectra of the input X radiation,

Wout (u): the noise power spectra of the linearised detector output signal.

The W_{in} parameter is given by the multiplication of the air Kerma (K_a) with the squared signal-to-noise ratio SNR_{in}^2, that depends on the X-ray energy spectrum:

$$W_{in} = K_a \cdot SNR_{in}^2$$

The W_{out} output noise power spectrum parameter is evaluated from the centred region (~125 mm x 125 mm in size) of uniformly exposed images.

The measurement equipment for the DQE is based on the standard of IEC 61267 [13] and the IEC 62220-1 [14] and it is consisted by three parts: 1) a tube unit, 2) a radiometric bench and 3) a support for the test object (Fig. **8**).

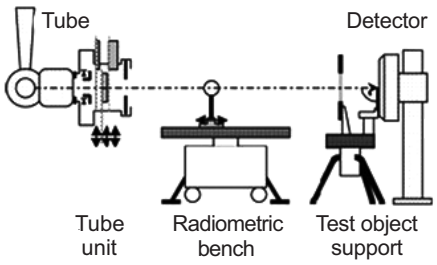

Fig. (8). Parts of the measurement equipment for the DQE [15].

The tube unit contains a set of aluminium filters in order to adjust the radiation quality, an adjustable diaphragm and a facility for monitoring the radiation output of the tubes. The radiometric bench is mainly used in order to measure the exposure level, featuring alignment and automatic positioning for the measurement of the photon fluence. Finally, the support for the test objet and the detector diaphragm is placed right in front of the detector unit. In case of vertical beam axis these two parts are placed on a bucky table just above the detector unit.

Illers H. *et al.* (2005) have conducted measurements on an Agfa CR system, with MD 30 image plate housed in a cassette during exposure. The image plate of this system was read by an Agfa Solo scanner with a pixel pitch of 113μm. The system was exposed to radiation ranging from ~1 to 20μGy with no other parts, such as AEC chamber or anti-scatter grid, used in front of the detectors. At the same exposure rate, measurments have been also conducted for the Kodak Direct View DR 9000 system, which uses a direct flat-panel detector of 500mm layer of amorphous selenium with a pixel pitch of 139mm. In the direct flat-panel detector system the anti-scatter grid and the cover plate were removed, but the AEC chamber was in place during the measurements. The inclusion of such layers will reduce the DQE due to additional absorption and scatter radiation.

The distribution of DQE of the CR detectors depends on the exposure and is best for the low-exposure level. As it is observed in Fig. (**9a**) the DQE is reduced significantly above ~10 mGy, which is due to the increasing importance of fixed pattern noise. However, the dependency on the radiation quality is more significant for the DDR than for the CR system and the DQE is best at the highest exposure levels. The dependence of DQE on the radiation quality and on the exposure level is important and should be considered carefully [15].

The DQE of various detectors (apart from Agfa) are shown in Fig. (**10**). The vertical y axis represents the DQE, while the horizontal x axis represents line pairs per mm (lp/mm), which is the inverse of spatial size and so higher lp/mm represent smaller size objects in the image. A DQE of 100% would represent perfect dose efficiency, but this does not happen as the final signal is enriched with the noise provided by the detector. In addition, the dose efficiency gets poorer as the objects get smaller (as the lp/mm increases).

The Kodak MinR-2000 is a common screen-film system and therefore can be considered as a reference point. From Fig. (**10**) it is well presented that Fuji CR has a DQE, or dose efficiency, exceeding screen-film for the largest objects (small lp/mm) while above about 2 lp/mm, it is inferior. In the case of the GE detector the DQE (that is based on cesium iodide) becomes inferior to screen-film for the highest spatial frequencies. Finally, in the Hologic Selenia system the DQE exceeds of all the others by a significant margin and in that way the image quality is superior at a match dose and can give a better image then the other systems at lower doses.

In practice, because the measurement of the DQE is very time consuming, it can be followed a simple procedure. An ionization chamber is placed in the center of the beam at a distance of FDD=1m and then the collimator is adjusted in order that the field covers the whole detector. At the exit of the tube a filter of copper (Cu), 1mm thick, is used. The tube voltage remains constant at 70kVp (with as small deviation as possible) while the value of the mAs changes manually. Each measurement is recorded and compared to a reference one that is given by the international standards, and should not differ more than 20% from each other [16].

5. ENTRANCE SURFACE DOSE

The entrance skin dose (ESD) is the absorbed dose in the skin at a given location on the patient. It includes the backscattered radiation from the patient, which contributes 27-45% to the measurement and is affected by the focus to skin distance (FSD), the field size and the chamber position. The calculation of ESD can be done with the use of an ionization chamber, that is placed on the surface of a tissue equivalent phantom (e.g., a polymethyl-methacrylate-

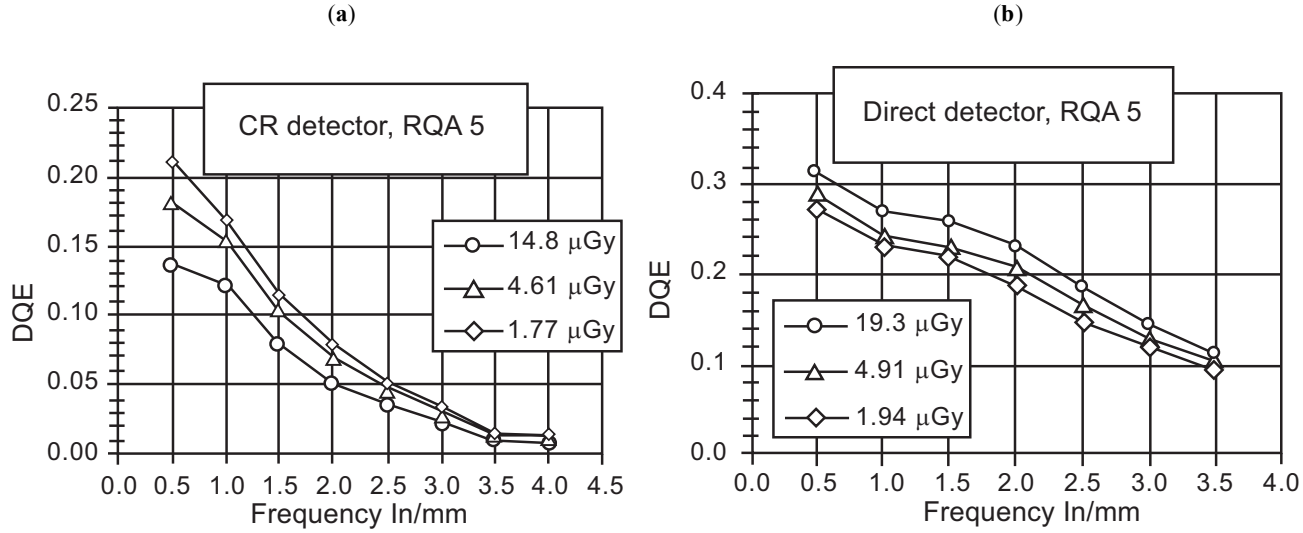

This figure was taken from the review of H. Illers *et al.* (2005).

Fig. (9). Distributions of the DQE (**a**) of the Agfa CR system with MD 30 imageplate, flying spot scanner 'Solo' for RQA 5 and (**b**) of the direct detector for RQA 5 [15].

PMMA phantom), in order to measure the in-air exposure at several x-ray tube kilovoltages covering all the clinical range. The results are expressed as exposure per milliampere second (mR/mAs, or mGy air kerma/mAs) [17].

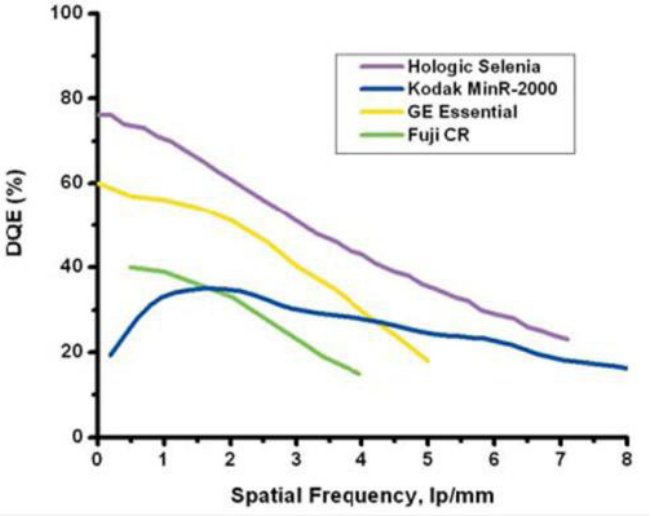

The results that are desposed refere to Fuji CR film, screen-film (Kodak), cesium iodide (GE), and selenium detectors (Hologic) [16].

This figure was taken from the paper of A. Smith (2006).

Fig. (10). Dose efficiency as shown by the distribution of Detective Quantum Efficiency for different types of films.

According to C.J. Martin (1995), an alternative approach is to measure the incident dose rate, which can be related to dose area product, by using a copper phantom, as it gives similar incident dose rates as Perpex, under automatic gain control. This method allows measurements of incident dose rate that are made by using copper to be linked to corresponding thicknesses of tissue-equivalent material and because only a few millimeters of copper are required, contributions from backscatter can be minimized. Finally the entrance surface dose can be derived by using the backscattered factor and in that way the patient dose is reduced [18].

Another well known method to measure the ESD while reducing the patient dose is to measure the radiation of the whole beam and then multiply the result with the backscattered factor of the material of the phantom (or of the soft tissue factor). For the measurement of the whole beam, estimating of the dose-area product (DAP) is demanded. The water is equivalent to soft tissue so, numerical differences between the air kerma and the water kerma based backscatter factors are insignificant for low energy photons, thus, the DAPs could be multiplied to the B_{air} or the B_w factors [19].

Although the use of low tube potentials is often recommended by the manufacturers of digital systems, this will lead to less penetrating beams and hence to possibly higher doses. Therefore, clinically diagnostic images can be achieved by using high tube potentials and lower mAs. In that case, the patient dose is reduced, but the contrast of the image is reduced, as well [20].

According to N.W. Marshall (2009), high tube potentials can be used to obtain low skin doses for a given examination. This is based on the fact that the beam has greater penetration in the phantom and leads to lower mAs values and, as a result of this, to lower ESD. The phenomenon happens when the air kerma at the CR cassette is constant, and the results are shown to the Fig. (**11**). The results for the constant CNR show that the ESD is approximately independent of tube potential, but a higher CNR would increase ESD at all tube potentials. Somehow the ESD is a simple measure of risk and these results could be expanded further by examining the depth dose in the phantom or even the effective dose for a range of examinations [21].

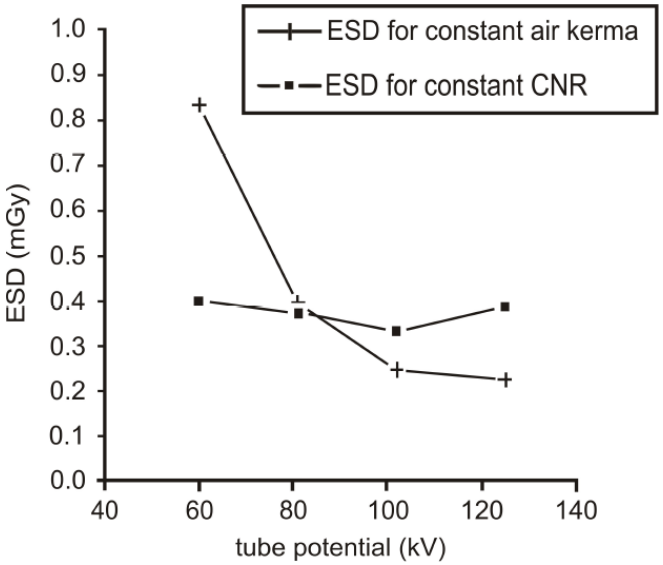

This figure was taken from the article of N. W. Marshall (2009).

Fig. (11). Entrance surface dose (ESD) measured at the input to the 20 cm tissue equivalent phantom for the constant air kerma at the CR cassette (~ 3 μGy) and for the constant target CNR method [21].

A research made by G Compagnone *et al*. (2006) has shown that the ESD in CR is greater than in DDR in different kind of examinations. The results of the research are shown in Table **1**.

Table 1. Entrance Surface Dose (ESD) for Standard Radiographic Examinations*

Examination and Projection	ESD_{CR} (mGy)	ESD_{DDR} (mGy)	ESD_{DDR} - ESD_{CR} (%)
AP Abdomen	2,4	1,64	-32
PA Chest	0,11	0,06	-45
LAT Chest	0,2	0,13	-35
AP Lumbar Spine	2,54	1,16	-54
LAT Lumbar Spine	5,39	1,72	-68
LAT Lumbo-Sacral Joint	5,39	1,72	-68
AP Pelvis	1,83	1,02	-44
AP Skull	1,61	1,58	-2
LAT Skull	1,11	0,89	-20
AP Urinary track	2,51	N/A	N/A

Abr: AP, anteroposterior; PA, posteroanterior; LAT, lateral.
*Compagnone G *et al*. 2006 [20].

As it is depicted in Table **1**, DDR results in lower ESDs than those in CR. A possible reason for this is that in CR systems are used higher tube potential techniques than DDR systems. Hence, it occurs that DDR is a preferable method as far as ESD is concerned [20].

6. RADIATION OUTPUT RATE DOSE

The tube output is determined by the ratio of the entrance surface dose (mGy) and the focal spot charge (mAs). According to IAEA [22] and the ACPSEM [5] a high radiation output is desirable to ensure that the exposure times are sufficiently short to minimize the patient's movements and discomfort.

In the ACPSEM protocol [5] is reported that rather than measuring the output rate it is more sufficient to measure the exposure time, or observe the required mAs, under automatic exposure control (AEC) conditions. This is made by using a 6cm PMMA phantom, or any phantom equivalent to soft tissue, under AEC operation using clinically relevant technique factors (kVp, anode/filter combination etc.) that must be consistent with those used in the assessment of the CNR and the MGD. According to that protocol the exposure time for the best function of the operation, should be less than 3.5sec and 2 sec (for CNR and MGD respectively). On the other side, IAEA does not base the measurements of the radiation output rate on the time exposure [22].

In this stage of the QC the kVp's accuracy and repeatability are checked. The methods that are used in this step for the DR are the same as for the classical radiography. To measure the radiation output, the beam is collimated and it is used a calibrated air ionization chamber, which usually includes the effect of backscattered radiation, and a PMMA (or Plexiglas) phantom of 20cm. It could also be used any phantom that is equivalent to soft tissue. As shown in Fig. (**12**), the chamber is placed at the center of the radiation field and on the surface of the phantom (the focal to film distance-FFD is constant) and it is connected with an electrometer that has a direct readout. In case that the ionization chamber does not include the effect of the backscattered radiation, a thin layer of lead is placed between the chamber and the table.

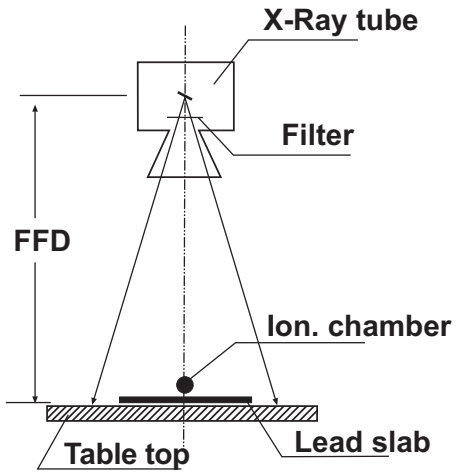

Fig. (12). Arrangement for radiation output measurement [22].

To make the measurements the rate of the mAs is kept constant (or with as small diviations as possible) and the voltage (kV) is changing with fixed intervals.

7. REPRODUCIBILITY

In order to control the reproducibility of the radiation output, and hence the entrance surface dose, ten consecutive measurements should be taken at the same FFD within a time period of one hour, for any combination of operating loading factors (kVp and mAs). The coefficient of variation (CV) of each one of the measurments should not be greater than 0.05 and the rate of eachone of them should not be greater than 15% of the mean value of the ten measurments.

To calculate the CV it is used the ratio of the standard deviation to the mean value of a series of measurements, which is appeared in the following equation:

$$CV = \frac{S}{\overline{X}} = \frac{1}{\overline{X}}\left[\frac{\sum_{i=1}^{n}(X_i - \overline{X})^2}{n-1}\right]^{1/2}$$

where,

CV: is the coefficient of variation,

S: is the estimated standard deviation,

X_i: is the value of the ith measurement;

$\overline{X}$: is the mean value of the measurements; and n is the number of measurements.

8. LINEARITY

In order to check the linearity of the radiation output, the x-ray tube voltage (kV) is kept contsant while the range of the mAs is varying. The procedure is repeated for two different FFD distances. The quotient of the average air kerma measurement divided by the indicated current time product obtained at the two applicable settings must not differ more than 0.10 rimes the sum of the measurments:

$$| X_1 - X_2 | \leq 0.10(X_1 + X_2)$$

where, X_1, X_2 : the quotients of the average air kermas measurement divided by the current time product at two applicable settings of X-ray tube current or X-ray tube current-time product [23].

9. IMAGE QUALITY CONTROL

In medical imaging, validation of image quality is a major concern. The diagnostic value of the image is defined by its degree of quality. Various parameters should be tested in order to define the quality of a medical image.

9.1. Phantoms

In order to facilitate image quality control procedures, a variety of test objects or phantoms have launched by diverse organizations. These test objects simulate parts of the human body (have approximate attenuation x- ray coefficients in the energy spectrum used clinically) and are sensitive to changes in imaging performance. There are many test objects which are different as far as material, dimensions, form, shape, contrast and size of the details are concerned. The selection of the test object depends on the imaging task, the sensitivity and the precision required for discriminating changes in imaging performance. Some of the most known phantoms

utilized nowadays in Digital Radiography (DR) are presented. Test objects TO20, TO16, TO12 and TO10 (Fig. **13**) are designed for quick quantitative assessments of image quality. The TO20 test object is intended for use with Digital Subtraction Fluoroscopy and it consists of 144 details (12 sizes x 12 contrasts). The size of the details ranges from 11mm to 0.25mm and the contrast range is 0.0014 to 0.924 at 75kV, with a 1.5mm Cu filtration. TO16 is intended for use with Computed Digital Radiography and it owns the same features as TO20. TO12 is intended for use with Digital Spot Imaging Systems and it consists of 108 details (12 sizes x 9 contrasts). The size of the details ranges from 11mm to 0.25mm and the contrast range is 0.0043 to 0.954 at 70kV with 1.0mm Cu filtration. TO10 is intended for use with Fluoroscopy systems and it consists of 108 details (12 sizes x 9 contrasts). The size of the details ranges from 11mm to 0.25mm and the contrast range is 0.012 to 0.930 at 70kV with 1.0mm Cu filtration [24].

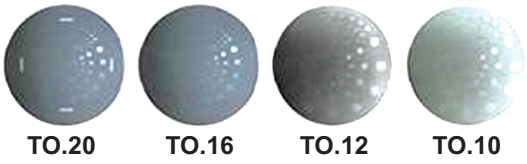

Fig. (13). TO20, TO16, TO12 and TO10 test objects for quality control of Digital Radiographic systems [24].

A contrast- detail (CD) phantom tests the observer's perception. With a CD-phantom it is possible to quantify both, details and contrasts, as observed by the radiologist. The CDRAD 2.0 phantom can be used within the entire range of diagnostic imaging systems, such as fluoroscopy and digital subtraction angiography while the CDMAM 3.4 is used particularly in mammography systems. Image quality is measured simply by counting the number of details detected and the number of bar- patterns resolved in the image. CDRAD 2.0 and CDMAM 3.4 enable the following checks to be made: sensitometric measurements (10 test point details, 5.6mm diameter), resolution limit (0.5 to 14.3 lp/mm), low contrast large detail detectability (17 details, 11mm diameter) and high contrast small detail detactability (17 details, 0.5mm diameter). The CDRAD 2.0 phantom consists of a Plexiglas tablet with cylindrical holes of exact diameter and depth (tolerances: 0.02 mm). Together with additional Plexiglas tablets, to simulate the dimensions of the patient, the radiographic image of the phantom gives information about the imaging performance of the whole system. The Fig. (**14**) shows 225 squares, 15 rows and 15 columns. In each square either one or two spots are present, being the images of the holes. The first three rows show only one spot, while the other rows have two identical spots, one in the middle and one in a randomly chosen corner. The optical densities of the spots are higher as compared to the uniform background. Due to the (exponentially) increasing depth of the holes in horizontal direction, the image shows 15 columns of spots with increasing contrast. In the vertical direction the diameter of the holes increases stepwise and exponentially from 0.3 to 8.0 mm. For the image this means 15 rows of spots with increasing spatial resolution. The CDMAM 3.4 phantom consists of an aluminium base with gold discs of various thickness and diameter. The aluminium base is attached to a Plexiglas (PMMA) cover. The phantom is delivered with 4 PMMA plates of each 10 mm thickness. Every plate has an engraved marker with lead inlet for identification. The gold discs are arranged in a matrix of 16 rows by 16 columns. Within a row the disc diameter is constant, with (partly) logarithmic increasing thickness and within a column the thickness of the discs is constant and the diameter increases logarithmic. Each square contains two identical discs (same thickness, same diameter), one in the centre and one in a randomly chosen corner. Easily recognizable patterns have been avoided. The total matrix is rotated by 45 degrees and the corners of the matrix are skipped. This is done for two reasons, getting a better focus on the interesting part (low contrast, small diameter) and making the recognition of the patterns more difficult [25].

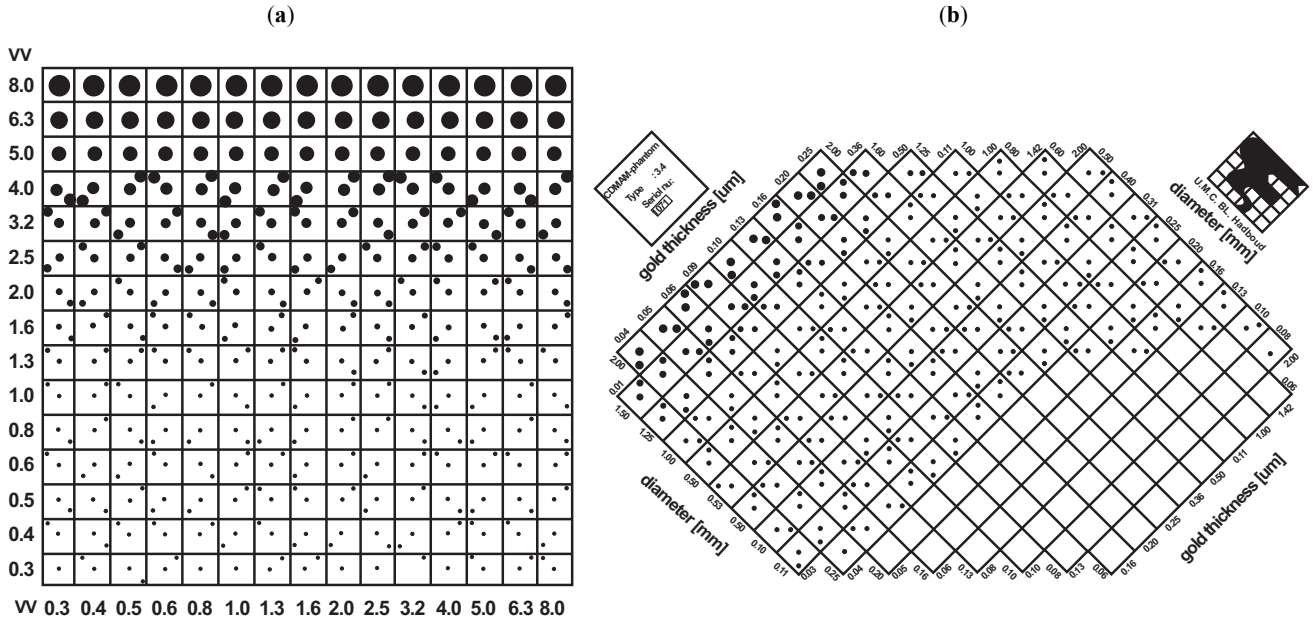

Fig. (14). Contrast- Detail phantoms for Digital **a**) Radiography (CDRAD 2.0) and **b**) Mammography (CDMAM 3.4) [25].

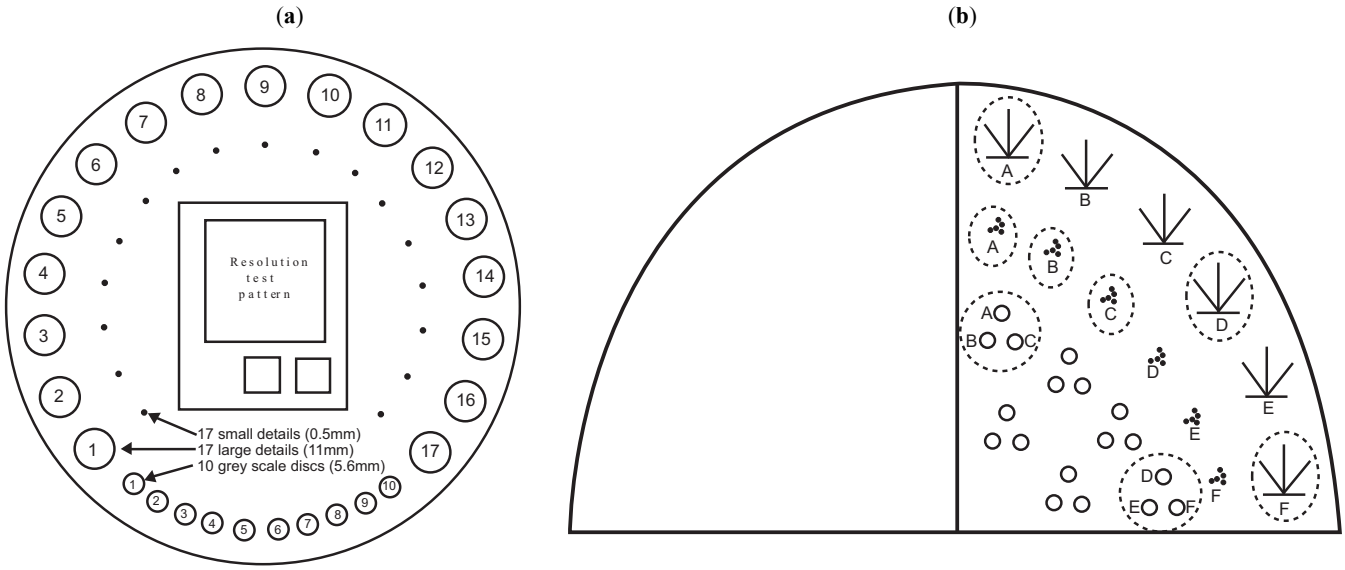

Fig. (15). Phantoms for quality control in digital a) Radiographic (TOR RAD) or b) Mammographic (TOR MAM) systems [24].

Another test object that is used for routine quality control of digital radiography (or mammography) is TOR CDR (or TOR MAM). These test object enable the following tests to be carried out: film density measurements (base and fog, speed index, contrast index), low- contrast sensitivity (large details), high- contrast sensitivity (small details) and spatial resolution limit. The test details of TOR CDR and TOR MAM are shown in the Fig. (**15**). TOR MAM phantom is divided into two halves, with one half (left) containing simulated breast tissue, and the other containing particular features representative of those found in breast tissue: filaments, particles and disks. Each feature has levels A–F which correspond to decreasing relative thickness, size, and contrasts for the filaments, particles and disks respectively [24].

9.2. kVp Performance

The image quality as well as the patient dose is depended on any variation in the generator kilovoltage (kV) of the x-ray set, the anode material and the filtration, and therefore an accurate kV calibration is required for the accuracy and the reproducibility of the tube and the uniformity of the detected signal. According to "The European Protocol for the Quality Control of the Physical and Technical Aspects" as well as to the IAEA, every six months, should be performed a non-invasive tube voltage check for the whole kV-range that is used. The equipment that is being used for this type of control is an electronic device (multi-function meter) in order to measure the time, the dose and the kVp. These exposures should be made using a kVp and target/filter combination that is in routine clinical use [5, 23].

9.3. Accuracy

The tube voltage should be checked for the whole range of kV that is used, with intervals of 1kV. The measured kVp shall be within ±5% of the specified value over the clinically relevant range. In order to effectuate the measurements, a meter is set at about 100cm from the focus of the anode, or as it is prescribed by the manufacturer. The intension is set ~20mAs and remains as constant as possible. After the measures have been taken, the errors-differences between set and measured values are being calculated and should be within ±5% [5, 26].

9.4. Repeatability

This parameter is also found as reproducibility and in order to assess the repeatability of kVp is recommended a minimum of four manually selected exposures while the range of kV is fixed (usually at 70kV) and the error area is within ± 0.5kV. These exposures should be made using a kVp and target/filter combination that is in routine clinical use. According to C. Walsh (2008), a plate of 21mm Al that is supplied as standard to the system should be mounted at the tube head. The measurements chamber (ionisation chamber) should be placed on the table or at the face of the chest detector. The distance between the source and the image (SID) should be 150cm for the chest detector and 110cm for the table detector. After the measurements have been taken, the CV is being calculated and should not exceed 0.02 [5, 27, 28]. The calculation is been made by:

$$CV = \frac{SD}{mean}$$

where,

SD: standard diviation

Mean: the mean value of all measurments

9.5. Dose Detector Index (DDI)

It is a numerical value displayed with each exposure that correlates to dose. It must be noted that the DDI does not necessarily indicate that the examination has had the correct exposure parameters set but does suggest that the image plate has received an appropriate exposure. Each manufacturer has a specific method for providing this indicator, but the relationship between its value and the exposure value is known (Table **2**) [29]. The variation of the DDI should be less than 5%.

Table 2. DR Exposure Indicators, Units, and Calibration Conditions

Manufacturer	Indicator Name	Symbol	Units	Exposure Dependence	Calibration Conditions
Fujifilm	S Value	S	Unitless	200/S = X (mR)	1 mR at 80 kVp, 3mm Al (Total) = S = 200
Kodak	Exposure Index	EI	mbels	EI+300 = 2X	1 mR at 80 kVp, 1mm Al and 0.5mm Cu = EI = 2000
Agfa	Log of Median of Histogram	lgM	bels	lgM+0.3 = 2X	2.5 μGy at 75 kVp, 1.5 mm Cu = lgM = 1.96 at 400 Speed Class
Konica	Sensitivity Number	S value	Unitless	for QR = k 200/S α X (mR)	for QR = 200, 1 mR at 80 kVp = 200
Canon	Reached Exposure Value	REX	Unitless	for Brightness = c_1 Contrast = c_2 REX α X (mR)	for Brightness = 16, Contrast = 10, 1 mR ≈ 106
GE	Uncompensated Detector Exposure	UDExp	μGy Air KERMA	UDExp α X (μGy)	80 kVp, standard filtration, no grid
GE	Compensated Detector Exposure	CDExp	μGy Air KERMA	CDExp α X (μGy)	kVp, grid, and additional filter compensation
GE	Detector Exposure Index	DEI	Unitless	DEI ≈2.4X (mR)	Not Available
Swissray	Dose Indicator	DI	Unitless	Not Available	Not Available
Imaging Dynamics Company	Accutech	f#	Unitless	$2^{f\#} = X(mR)/X_{tgt}(mR)$	80 kVp, 1mm Cu
Philips	Exposure Index	EI	Unitless	100/S α X (mR)	RQA5, 70 kV, 21mm Al, HVL = 7.1mm Al
Siemens Medical Systems	Exposure Index	EXI	μGy Air KERMA	X (μGy) = EI/100	RQA5, 70 kV, 0.6mm Cu, HVL = 6.8mm Al
Alara CR	Exposure Indicator Value	EIV	mbels	EIV + 300 = 2X	1 mR at RQA5, 70 kV, 21mm Al, HVL = 7.1mm Al = EIV = 2000
iCRco	Exposure Index	None	Unitless	Exposure Index log[X (mR)]	1 mR at 80 kVp, 1.5mm Cu = Exp. Ind. = 0

* Willis CE. 2004 [29].

9.6. Uniformity

This parameter is also referred as "Homogeneity" and is very important because a non-uniform response could affect clinical image quality. It is generally agreed that the evaluation of the image receptor uniformity should be undertaken routinely. However, there are some differences as to the methodology, but in all cases is used an image of a standard PMMA test block (phantom) that must be free of imperfections, scratches, dust and dirt and that is covering the entire image receptor. As another material of the phantom, Plexiglas could be used, as well. According to the KCARE Protocol [6, 30, 31], the measurements are taken by placing an ionization chamber on the couch at 1 - 1.2m from the focus and at least 30cm above the table (the actual distances must be recorded) and centred in the x-ray beam. The collimation is then set to cover the entire detector. A filtration of 1.0mm of copper is placed at the tube head and the chamber is exposed to at tube voltage that depends on the CR system (the type of cassette that is used) as shown in Table **2**. The mAs should be set manually such that the inverse square law corrected dose to the table level is approximately 10 μGy. The exposure is required to be repeated twice, under the same parameters, and before the second exposure the plate is rotated 180° about the vertical axis so that the non uniformities can be prevented due to the anode heal affect. After the exposure the plate of the cassette is being read without a time delay between exposures and read out. The parameters that are set depend on the type of the system-cassette.

The next step is to check the image for non-uniformity and artefacts and after that five ranges of interest (ROI) are defined on the image (Fig. **16**). For Fuji, Konica and Kodak systems where ROI analysis is not available, read uniformly exposed plates using the FIX mode the images should be print onto laser films. On the film there are defined five ranges of interest (ROI), one centrally located and the other four placed near the corners of the image, the size of which should be of order 10000 pixels. In every ROI is measured the optical density (OD) and the mean pixel values (PV).

On the other hand, for Agfa systems the Scanned Average Level (SAL) values, obtained from ROI analysis on the review workstation, should be used and there is no need to

print the image. From the measurements that have been taken, in order to consider the existence of uniformity, the maximum variation in the optical density of the five ROI should be less than 10% of each other. ACPSEM protocol [5] also follows the same course of action for settings as the KCARE; however, the evaluation is restricted to a smaller number of ROIs. According to this protocol only three ROIs are placed in a line parallel to the chest wall to avoid issues associated with the heel effect. In these ROIs, the mean pixel value (PV) is measured and should not differ more than 10% between them.

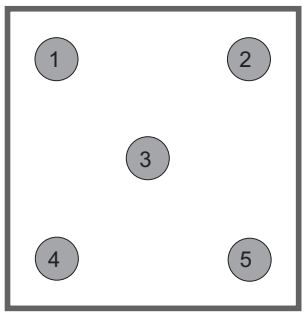

Fig. (16). Positions of the ROIs for uniformity tests.

As far as DDR systems are conserned, the same exposure conditions are followed. The uniformity of the detector can be assessed directly by visual inspection of the images for non-uniformities or by calculating the PV in a region of interest if supported by the software, as in CR systems.

9.7. Linearity

Linearity determines the response of the detector and readout systems to the exposure variation. AAPM protocol suggests that a calibrated radiographic x-ray tube with reproducible output (kV accuracy better than $\pm 5\%$ and exposure output accuracy $\pm 2\%$) and acquisition geometry/detector orientation must be maintained. The proposed technique is 80 kVp, 180 cm SID, and 0.5 mm Cu + 1 mm Al filtration, with the beam collimated just outside the total detector area. Radiographic techniques are determined in order to provide incident exposures of approximately 0.1, 1.0, and 10 mR. Actual incident exposure should be measured with a calibrated ionization chamber free-in-air (no backscatter) and calculated to the surface of the detector. For each incident exposure, three independent images should be acquired, and a fixed delay time of 10 minutes between exposure and processing should be used. KCARE protocol suggests a focus-to-detector distance at 150 cm and the proposed technique is 70kVp with 1.0mm Cu at the tube head to deliver doses of order 1μGy, 4μGy, 12μGy and 50μGy. On the other hand, ACPSEM protocol utilises a 40-mm thick PMMA block which should cover at least the central part of the detector. A clinically relevant kVp and target/filter combination is arranged as well as the range of mAs values selected should cover the clinically useful range (e.g. 5 to 500 mAs). The entrance surface air kerma (ESAK) is measured by placing a dosimeter in a position that will not influence the subsequent image measurements. Images are viewed and a ROI is drawn centrally along the long axis and approximately 40 mm from the chest wall. The mean pixel value (MPV), with pixel offset value subsequently subtracted, and standard deviation (SD) are recorded. For digital systems plots of mean pixel value and SD^2 against the ESAK are drawn and linearity tested by noting the square of the correlation coefficient (R^2). According to ACPSEM protocol, reasonable specification is to require that the plot of mean pixel value and SD^2 versus ESAK should have $R^2 > 0.99$ and $R^2 > 0.954$, respectively while KCARE protocol suggests that the trend-line plotted should have an R^2 fit value >0.95. The difference between DDR and CR systems is that in CR systems the response to air kerma variations depends on the system. In all cases the exposure indicator is recorded for each image, which must be acquired with the same cassette on each occasion. It is simpler to confirm linearity by examining the dependence of the exposure indicator on the ESAK [3, 30, 32, 33].

9.8. Threshold Contrast Detail Detectability (TCDD)

This parameter characterizes the detectability of a low-contrast object, and is influenced by several factors, including the object size, contrast between the object and the background, image noise and the system's modulation transfer function (MTF). The evaluation of the minimum discernible contrast to characterize the low-contrast resolution is generally performed in a subjective fashion on a test phantom with a low contrast resolution pattern. According to the AAPM a calibrated low-contrast test object such as the Leeds phantom designed for computed radiography or the UAB low-contrast phantom are appropriate for use, as are others. For the Leeds phantom setup (e.g. TO.12), 0.1, 1 and 10 mR, at 75 kVp beam with 1 mm added Cu filtration is used with a standard clinical acquisition protocol [34, 35]. The ACPSEM, likewise, utilizes the CDRAD 2.0 phantom (or CDMAM 3.4 phantom for mammography) with the same exposure parameters. On the other hand, KCARE utilizes TO20 (or TOR RAD or TOR CDR or equivalent) test object and quantifies the result of the test, having the same exposure conditions as AAPM and ACPSEM. The quantification happens by estimating the image quality factor (IQF) defined as:

$$IQF = \frac{1}{n}\sum_{i=1}^{n}\frac{H_T(A_i)}{H_T^{ref}(A_i)}\left[\frac{D_{ref}}{D}\right]^{0.5}$$

where,

$H_T(A)$ = threshold contrast detail index values calculated from the image,

$H_{Tref}(A)$ = threshold contrast detail index values calculated from a reference image of a system known to be in good adjustment

D = the dose to the image plate

D_{ref} = the dose to the image plate for the reference image

n = the number of details in the test object.

The IQF could be compared to those from other similar systems and it is useful for future QA tests.

9.9. Image Noise

Image noise is primarily determined by the dose setting of the x-ray tube, the detector efficiency and the reconstruction algorithm. The noise of the CR system is tested by acquiring three images of a low-contrast phantom,

using 0.1, 1 and 10 mR, at 70 kVp beam with 1 mm of Cu filtration. The phantoms that are utilized are the same as in TCDD. The noise is quantified by the standard deviation of the pixel value in a fixed small region of the image (PVSD). The logarithm of noise is linearly dependent on the logarithm of exposure (E):

$\log(PVSD) = a + b \log e$

with a correlation coefficient >0.95.

9.10. Limiting (spatial) Resolution/Resolution Uniformity

Spatial resolution tests include measurement of the central and peripheral limiting resolution for each IP size and type (standard and high resolution) along the scan and sub-scan directions, and a third at 45° direction (R_{hor}, R_{ver}, $R_{45°}$). To determine consistency of the resolution response across the IP, use a fine wire mesh pattern. An inherent limitation of all forms of magnification radiography is the finite size of the X-ray focus, causing geometric blurring of an imaged object edge. The spatial resolution in digital radiography systems is also limited by the Nyquist frequency of the detector defined by $(2p)^{-1}$ where p is the pixel size [36]. The high contrast resolution test patterns (e.g. Huttner line-pairs test object, TOR CDR, TOR RAD, TOR MAM) consist of various lead thicknesses and each test pattern is enclosed in plastic. The exposure conditions are: 5 mR incident exposure with an unfiltered 50- 60 kVp beam at 180 cm SID (Source to IP distance). The limiting resolution is determined by inspecting the finished radiograph with a 5 - 10 power magnifying glass. This is achieved by looking for the last bar section in which a clear distinction between line and space can be observed. The number corresponding to this line pair section represents the line pair resolution for the system. The qualitative criteria that must be met are: wire mesh image should be uniform and free of any blurring across the image while the quantitative criteria are: $R_{hor} / f_{Nyquist} > 0.9$, $R_{ver} / f_{Nyquist} > 0.9$ and $R_{45°} / (1.41\ f_{Nyquist}) > 0.9$. Moreover, the measured resolution should be within 10% of the theoretical resolution based upon the sampling frequency of the imaging plate as specified by the manufacturer. According to ACPSEM, the MTF is recognised as the best indicator of equipment system resolution under the condition that the appropriate software does exist. The MTF of an imaging system is defined as the absolute value of its optical transfer function, normalized to unity at spatial frequency zero. One of the established methods to determine the MTF is based on the use of a sharp edge that is imaged to produce an edge spread function (ESF). The ESF is then differentiated to obtain the line spread function (LSF), from which the MTF is calculated by a Fourier transform. An edge test device with a well-defined edge is usually realized by carefully machining a thin piece of metal, (e.g. lead, tungsten, or platinum). Material thicknesses of 0.1 to 0.25 mm are often used to allow easy manufacturing and handling as well as accurate alignment of the edge in the x-ray beam. Depending on the actual thickness of the material and on the beam quality used for imaging, the metal sheet may be either (almost) fully absorbing or semitransparent [37]. Every manufacturer usually has specific instructions for the acquisition of the MTF.

9.11. Spatial Accuracy/Spatial Linearity/Laser Beam Function

A convenient way to observe any spatial non-linearity and geometric distortion is to image a film/screen contact mesh pattern with light compression. The mesh may need to be placed asymmetrically on the imaging device (to avoid Moiré effects in the image). The image is viewed in magnified mode using magnify and roam tools and any distortion is readily evident, although the assessment is somewhat subjective. Spatial distance accuracy is referred to the confirmation of the system distance callipers, and hence pixel size. It is determined with "x-ray" ruler lead markers or from flat objects with known dimensions such as a resolution bar phantom. Laser Beam Function control is referred to the assessment of laser beam scanline integrity and jitter and it is also determined with "x-ray" ruler lead markers like spatial accuracy. The exposure conditions are the same as in Limiting Resolution/ Resolution Uniformity and the procedure is repeated for all available image plate resolutions. The measured distances should be within 2% of actual. To minimise any magnification effects, the rulers should be placed in direct contact with either the detector or a CR cassette, depending on the circumstances, unless otherwise indicated by the system manufacturer. As far as the laser beam function is concerned, a narrow window width is selected, such that the image appears largely polarised to black or white. This should allow the edge to be easily differentiated from the background. When examining the edge of the ruler in the image, it should be continuous across the full length of the image. Stair step characteristics should be uniform across the length of the image. Regions of over or undershoot of the scan lines indicate a timer or laser beam modulation problem.

9.12. Erasure Thoroughness

The imaging plate (IP), if is improperly or insufficiently erased, can potentially give rise to image artefacts. The test of the erasure capability is performed by exposing an erased IP (unused for 1 h before the test) at high exposure levels (50 mR) with a centrally placed high-contrast test object (a thick lead block), reading the plate and re-exposing the plate to a uniform incident exposure of about 1 mR. The re-exposed image should be free from ghost artefacts. The ghost signal is quantified in our software by the percentage difference between the average pixel value in the region previously occupied by the high-contrast object and in the surrounding area. The percentage difference between the mean pixel value in the region previously occupied by the high-contrast object and the surrounding area should be less than 2%. According to KCARE protocol, erasure cycle efficiency is measured by positioning a plate on the table at ~1.5 m, setting a 10 cm x 10 cm field and placing a piece of attenuating material (e.g. Copper or lead) at the centre of the CR plate. Then, it is exposed at 80kVp, 25mAs with no filtration. After reading and erasing, the plate is re-exposed with a 9 cm x 9 cm field centred on the same point on the plate, with no attenuating material in place, using 80kVp, 0.5mAs and no filtration. If a remnant is visible, a region of interest analysis is used to quantify the difference in pixel value between the ghosted and unghosted areas. There

should be <1% (remedial) difference between the System Transfer Properties (STP) corrected pixel values in the ghosted region and the surrounding areas [30, 38]. In DDR systems this control is omitted, due to the use of flat panel or solid state detectors.

9.13. Signal to Noise Ratio

Signal to noise ratio (SNR) is the quotient of mean value of the linearized signal intensity and SD of the noise (intensity distribution) at this signal intensity. By linearized signal intensity it is meant the numerical signal value of a picture element (pixel) of the digital image (MPV), which is proportional to the radiation dose. The SNR is a critical factor in all imaging modalities and is especially important in digital radiography. Image quality improves with higher SNR. In addition to the quantum noise from variations in a low dose x-ray beam, noise from the scintillation and electronic components of the DR system can decrease the SNR. SNR of a CR or DDR system depends on the dose (exposure time and conditions) at the detector, the radiographic system properties and it is also affected by the selection of the acquisition protocol. According to the European Commission, a 20-cm thick PMMA (or equivalent) phantom (or 2-cm thick for mammography) is imaged with aluminium object of 0.2 mm thickness and 10 x 10 mm^2 area, positioned on the top of PMMA layers which cover the entire detector area. In practice, the utilization of a plexiglass phantom instead PMMA yields similar results. Under AEC conditions the phantom is exposed. A similar procedure is followed for variable thickness of PMMA phantoms in the range of 2- 20 cm (or 2- 6 cm for mammography). In each case, the required additional PMMA thickness is added on top of a 0.2 mm Al object. SNR is calculated in a uniform image as a simple ratio of MPV and SD in a region of interest (ROI) approximately 1/3 the size of the image. ACPSEM protocol utilizes the ACR accreditation phantom for the evaluation of the medical image and defines the ROI approximately at 100 mm^2 measured using the workstation tools. The European protocol recommends a tolerance limit of $\leq 15\%$ of the baseline [32, 39-41].

9.14. Contrast to Noise Ratio

Even if the image has a high SNR, it is not useful unless there is a high enough contrast to noise ratio (CNR) to be able to distinguish among different tissues and tissue types, and in particular between healthy and pathological tissue. According to the European guidelines, the measurment of CNR is produced by 0.2 mm Al superimposed on variable PMMA thicknesses. PMMA layers are exposed by full automatic techniques [42]. ACPSEM protocol also suggests a uniform phantom with a test object of slightly varying attenuation which may consist of a PMMA sheet (ACR accreditation phantom) with either a hole test object, or uniform button like an aluminium foil of thickness 0.2 mm. Images of this test object are made with variable thicknesses of PMMA using AEC conditions just like in SNR measurements. In each image the MPV and SD, respectively are calculated for a ROI (~ 0.25 cm^2) located in a uniform part of the phantom (PV_{ph}, SD_{ph}) and in an area where the Al foil is located (PV_{Al}, SD_{Al}). The CNR is defined as:

$$CNR = \frac{MPV_{ph} - MPV_{Al}}{\sqrt{\left[\left(SD_{ph}^2 + SD_{Al}^2\right)/2\right]}}.$$

The European provisional specification requires that the CNR be at least 1.1 times and 0.9 times the CNR with 4 cm PMMA for 2 cm and 6 cm of PMMA, respectively. In some CR systems it may be difficult to extract meaningful statistics relating to ROIs because of the inadequacies of workstation software and the difficulty of linearising the data. Under these circumstances, the above test requirement on the CNR is waived and the performance must be assessed solely on the exposure indicator (EI) variation [5].

9.15. Automatic Exposure Control (AEC)

A well-designed AEC should be capable of modifying required detector exposures based on exposure conditions (typically selected kVP and mA) to compensate for energy dependence and exposure rate. Some of the factors that influence the AECs in digital radiography are the technique, the type of phantom and contributions from scatter. While AEC is an efficient method of obtaining homogeneous image quality, it may result in increased dose under certain circumstances. The variation and complexity of AEC facilities, even between systems supplied by the same manufacturer, can give rise to incorrect operation [43].

Computed radiography (CR) systems employ analogue mammography units, which are the same AEC systems as used in screen/film mammography, with the opportunity of adjusting AEC signal threshold to match the higher quantum efficiency of imaging plates over screen/film combinations. Direct radiography (DDR) systems use the digital detector itself as AEC sensor [42]. Many methods have been established to assess the AEC system's performance.

The AEC calibration for digital radiography systems requires an alternative parameter to optical density, ideally one related to the quality of a digital image. A good parameter for AEC optimization of DR systems is the square of CNR or SNR divided by the average glandular dose (AGD) [39, 42]. The calculations of CNR and SNR have already been mentioned above. AGD is determined as the mean dose received by the radiation sensitive tissue contained within the female breast and it cannot be directly estimated. For that reason, it is often estimated from the measurements of the breast entrance skin air kerma (BESAK) by applying a series of appropriate conversion factors. AGD is calculated for several thicknesses of PMMA (or equivalent) phantom like CNR [44].

Alternatively, the DDI could be used to determine the correct kV compensation curve required to calibrate the AECs for the loss in detector sensitivity with tube potential. DDI is calculated by maintaining the mAs, the phantom thickness and the dose to the surface of the phantom constant and altering the kVp. The variation should be less than 20% per kV. Another way to calculate DDI is to maintain mAs, kVp constant and change the thickness of the phantom or change the receptor dose [45, 46].

10. CURRENT AND FUTURE DEVELOPMENTS

Digital radiology is synonymous with image enhancement, rapid transmission to remote locations and

compact electronic storage. Continued development of digital radiography (CR or DDR) systems is spurred by radiology administrators' need for these advantages. The wide dynamic range provided by a digital system generates images with excellent diagnostic value.

Today, the emphasis in the development of digital technology revolves around the size of the hardware and the diagnostic quality of the images; in order to reduce the dose in the patient, without degrading the diagnostic value of the image. In the future, it is expected dramatic change in radiology, including widespread use of digital technologies.

Although digital radiography is a promising new approach for x-ray imaging system in diagnostic radiology, it is more complicated than conventional analogue approach. Hence, it is necessary to test these digital systems. Currently, various protocols exist for quality control of the physical and technical aspects of digital radiography with regard to image quality and radiation dose. Each protocol has specific advantages and disadvantages that must be taken into account in reporting the results. KCARE protocol is more easily applicable in clinical routine than the other protocols, as it contains simple steps for carrying out the quality control procedure. On the other hand, most of the tests are based on visual inspection and not in quantification of the results which renders the test less objective and not comparable to respective quality tests. AAPM protocol is a comprehensive protocol (especially for quality control of CR systems) which uses diverse indices, according to the manufacturer, for the quantification of the results. However, the most complete protocol for the quality control of digital radiography systems is the ACPSEM protocol as it contains detailed quality control tests that should be included in quality assurance (QA) programs.

Although, there are some individual efforts for creating quality assurance protocols in digital radiography, it is imperative to increase harmonisation as far as quality assurance and constancy checking is concerned, so as to compare the arising results among various systems. It is of outmost importance that the same parameters are measured using the same protocols, worldwide.

ABBREVIATIONS

AAPM	=	America's Association of Physicists in Medicine
ACPSEM	=	Australian College of Physical Engineers in Medicine
AEC	=	Automatic Exposure Control
AGD	=	Average Glandular Dose
CCD	=	Charged Couple Device
CNR	=	Contrast to Noise Ratio
CR	=	Computed Radiography
CV	=	Coefficient of Variation
DAP	=	Dose-Area Product
DD	=	Density Difference
DDR	=	Direct Digital Radiography
DDI	=	Dose Detector Index
DICOM	=	Digital Imaging and Communications in Medicine
DQE	=	Detective Quantum Efficiency
DR	=	Digital Radiography
EI	=	Exposure Indicator
ESAK	=	Entrance Surface Air Kerma
ESD	=	Entrance Surface Dose
ESF	=	Edge Spread Function
EUREF	=	European Reference Organisation
FDD	=	Focus to Detector Distance
FFD	=	Focus to (phosphor) Film Distance
FPD	=	Flat Panel Detector
FSD	=	Focus to Skin Diastance
GE	=	General Electric
GSDF	=	Grayscale Standard Display Function
IEC	=	International Electrotechnical Commission
IAEA	=	International Atomic Energy Agency
IP	=	Imaging Plate
IQF	=	Image Quality Factor
KCARE	=	King's Centre for the Assessment of Radiological Equipment
LSF	=	Line Spread Function
MD	=	Mid Density
MGD	=	Mean Glandular Dose
MPV	=	Mean Pixel Value
MTF	=	Modulation Transfer Function
OD	=	Optical Density
PACS	=	Picture Archiving and Communication System
PMMA	=	PolyMethyl-MethAcrylate
PSP	=	Photostimulable Storage Phosphor
PVSD	=	Standard Deviation of the Pixel Value
QA	=	Quality Assurance
QC	=	Quality Control
ROI	=	Region of Interest
RQA	=	Retail Quality Assurance
SAL	=	Scanned Average Level
SD	=	Standard Deviation
SID	=	Source to Image Distance
SNR	=	Signal to Noise Ratio
STP	=	System Transfer Properties
TCDD	=	Threshold Contrast Detail Detectability
TFT	=	Thin-Film Transistor

REFERENCES

[1] Zhao W, Andriole K, Samei E. In: Advances in Medical Physics 2006, Med. Phys. Pub., Madison, WI, 2006; 1-23.

[2] Katz N. Apparatus and method for supporting and shaping a photo-stimulable phosphor plate. US patent 20050029475, 2005.

[3] Warp RJ, Battle VP, Kump KS, Metz SW, Halsmer MA, Uppaluri R. Image pasting using geometry measurement and a flat-panel detector. US patent 6944265, 2005.

[4] Ravindran VR. Prelude to Digital Radiography. Indian Society for Non-Distructive Testing 2008; Available at: http://www.isnttvm.org/technical Details.jsp (18/12/2009).

[5] McLean ID, Heggie JCP, Herley J, Thomson FJ, Grewal RK. Recommendations for a digital mammography quality assurance program. Aust Phys Eng Sci Med 2009; 30(2): 65-100.

[6] King's Centre for the Assessment of Radiological Equipment Protocol for the QA of computed radiography systems, 2003; Draft 4.

[7] Digital Imaging and Communications in Medicine (DICOM), grayscale standard display function. National Electrical Manufacturers Association. 2003; Part 14. http://www.sciencedirect.com/science?_ob=RedirectURL&_method=externObjLink&_locator=url&_cdi=18104&_plusSign=%2B&_targetURL=http%253A%252F%252Fmedical.nema.org%252Fdicom%252F2003%252F03_14PU.pdf

[8] Krupinski EA, Williams MB, Andriole K, *et al*. Digital radiography image quality: image processing and display. J Am Coll Radiol 2007; 4: 389-400.

[9] Gray JE. Use of the SMPTE test pattern in picture archiving and communication systems. J Digit Imaging 1992; 5: 54-8.

[10] Jacobs J, Deprez T, Marchal G, Bosmans H. In: Digital mammography, initial results of the daily quality control of medical screen devices using a dynamic pattern in a digital mammography environment. Springer Berlin / Heidelberg 2006; 416-23.

[11] Lu ZF, Nickoloff EL, Terilli T. Dry view laser imager: one year experience on five imation units. Med Phys 1999; 26: 1817-21.

[12] Morgun ON, Nemchenko KE, Rogov YuV. Detective quantum efficiency as a quality parameter of imaging equipment. Biomed Eng 2003; 37: 258-61.

[13] International Electrotechnical Commission. Medical diagnostic X-ray equipment—radiation conditions for use in the determination of characteristics. IEC 61267. Second Edition, November 2005.

[14] International Electrotechnical Commission. Medical Electrical Equipment – Characteristics of digital X-ray imaging devices – Part 1: Determination of the detective quantum efficiency. IEC 62220-1. 1st ed. October 2003.

[15] Illers H, Buhr E, Hoeschen C. Measurement of the detective quantum efficiency (DQE) of digital X-ray detectors according to the novel standard IEC 62220-1. Radiat Prot Dosimetry 2005; 114: 39-44.

[16] Smith A. Image quality of CR mammography. Available at: http://www. hologic.com/data/W-BI-CR_11-06.pdf (*06/11/2009*)

[17] Goldman LW. Principles of CT: Radiation dose and image quality. J Nucl Med Technol 2007; 35: 213-25.

[18] Martin CJ. Measurement of patient entrance surface dose rates for fluoroscopic X-ray units. Phys Med Biol 1995; 40: 823-34.

[19] Omrane LB, Verhaegen F, Chahedn N, *et al*. An Investigation of entrance surface dose calculations for diagnostic radiology using monte carlo simulations and radiotherapy dosimetry formalisms. Phys Med Biol 2003; 48: 1809-24.

[20] Compagnone G, Casadio Baleni M, Pagan L, *et al*. Comparison of radiation doses to patients undergoing standard radiographic examinations with conventional screen–film radiography, computed radiography and direct digital radiography. Br J Radiol 2006; 79: 899-04.

[21] Marshall NW. An examination of automatic exposure control regimes for two digital radiography systems. Phys Med Biol 2009; 54: 4645-70.

[22] International Atomic Energy Agency (IAEA). Radiation protection in diagnostic and international radiology, IAEA Training material on radiation protection in diagnostic and interventional radiology; Part 19.4. http://rpop.iaea.org/RPOP/RPoP/Content/Documents/TrainingRadiology/Practicals/RPDIR-P19.04_kV_accuracy_WEB.ppt (*09/11/2009*)

[23] Radiation protection in radiology-large facilities, Safety Code 35: Safety Procedures for the Installation, Use and control of X-ray Equipment in large medical radiological facilities. minister of health of Canada, 2008 http://hc-sc.gc.ca/ewh-semt/pubs/radiation/safety-code_35-securite/section-b2-eng.php

[24] http://www.leedstestobjects.com/index.php#

[25] http://www.nuclemed.be/product.php?cat=123

[26] International atomic energy agency (IAEA). Radiation protection in diagnostic and international radiology, iaea training material on radiation protection in diagnostic and interventional radiology; Part 15.1, http://rpop.iaea.org/RPOP/RPoP/Content/Documents/TrainingRadiology/Practicals/RPDIR-P15.1_kVp_measurement_WEB.ppt (*09/11/2009*)

[27] Fitzgerald M, Heid P, Loon R, *et al.* The European protocol for the quality control of the physical and technical aspects of mammography screening. Third Edition, December 1999

[28] Walsh C, Gorman D, Byrne P, Larkin A, Dowling A, Malone JF. Quality assurance of computed and digital radiography systems. Radiat Prot Dosimetry 2008; 129: 271-5.

[29] Willis CE. Strategies for dose reduction in ordinary radiographic examinations using CR and DR. Pediatr Radiol 2004; 34: 196-200.

[30] King's Centre for the assessment of radiological equipment, Protocol for the QA of computed radiography systems, 2005; Draft 8.0.

[31] King's Centre for the Assessment of radiological equipment, Protocol for the QA of computed radiography systems, 2004 Draft 7.0.

[32] Report #116 of Task Group #116 of the AAPM, An exposure indicator for digital radiography, AAPM 2009.

[33] Samei E, Seibert JA, Willis CE, Flynn MJ, Mah E, Junck KL. Performance evaluation of computed radiography systems. Med Phys 2001; 28: 361-71.

[34] Cowen AR, Workman A, Price JS. Physical aspects of photostimulable phosphor computed radiography. Br J Radiol 1993; 66: 332-45.

[35] Wagner AJ, Barnes GT, Wu XZ. Assessing fluoroscopic contrast resolution: a practical and quantitative test tool. Med Phys 1991; 18: 894-99.

[36] Birch IP, Kotre CJ, Padgett R. Trends in Image Quality in High Magnification Digital Specimen Cabinet Radiography. Br J Radiol 2006; 79: 239-43.

[37] Neitzel U, Buhr E, Hilgers G, Granfors PR. Determination of the Modulation Transfer Function Using the Edge Method: Influence of Scattered Radiation. Med Phys 2004; 31: 3485-91.

[38] Rampado O, Isoardi P, Ropolo R. Quantitative assessment of computed radiography quality control parameters. Phys Med Biol 2006; 51: 1577-93.

[39] Muhogora WE, Devetti A, Padovani, Msaki RP, Bonutti F. Application of european protocol in the evaluation of contrast-to-noise ratio and mean glandular dose for two digital mammography systems. Radiat Prot Dosimetry 2008; 129; 231-6.

[40] Zoetelief J, Soldt RTM, Suliman II, Jansen RTM, Bosmans H. Quality control of equipment used in digital and interventional radiology. Radiat Prot Dosimetry 2005; 117: 277-82.

[41] Alexia L. Digital radiography in equine practice. Clin Tech Equine Pract 2004; 3: 352-60.

[42] Gennaro G, Golinelli P, Bellan E, *et al*. In: Automatic Exposure control in digital mammography: contrast-to-noise ratio versus average glandular dose. Springer Berlin / Heidelberg 2009; 711-15.

[43] Walsh C, Larkin A, Dennan S, Reilly G. Exposure variations under error conditions in automatic exposure controlled flm–screen projection radiography. Br J Radiol 2004; 77: 931-33.

[44] Beckett JR, Kotre CJ. Estimation of mean glandular dose for mammography of augmented breasts. Phy Med Biol 2000; 45: 3241-52.

[45] Doyleand P, Martin CJ. Calibrating automatic exposure control devices for digital radiography. Phys Med Biol 2006; 51: 5475-85.

[46] Doyle P, Gentle D, Martin CJ. Optimising automatic exposure control in computed radiography and the impact on patient dose. Radiat Prot Dosimetry 2005; 114: 236-39.

Received: December 9, 2009 Revised: January 15, 2010 Accepted: February 17, 2010